

FRACTURE RESISTANCE OF CRACKED WELDED JOINT

T. Adžiev*, J. Gočev*, S. Cvetkovski*, S. Sedmak**

Fracture mechanics tests performed on small-size specimens, tensile panels and full-scale pressure vessels have shown the possibility to predict residual strength of cracked pressure vessel by testing of small specimens. Critical region of HAZ, through which crack developed during tests, was analyzed by metallographic analysis. It was found that post-welding heat-treatment for residual stress relieving did not change significantly basic properties and microstructure.

INTRODUCTION

The analysis of residual stresses in welded joints was performed on microalloy steel weldments in cracked full-scale pressure vessels, tensile panels and small-size specimens (1-4). It is expected that in a real structure crack would occur in most critical location. In order to simulate situation in real structure, crack tip in the welded samples was located in the region of high residual stresses along welded joints axis in heat-affected-zone (HAZ). For sharp initial crack in homogeneous material pure mode I stress field operates ahead a crack tip and crack develops adopting the shape close to semi-circular with loading increase. However, situation is more complex in welded joint due to heterogeneity of its structure (5). Semi-circular crack shape in welded joint can be achieved if its constituents exhibit similar mechanical properties (6), but it is not the case. Welded joints are characterized by large scale of microstructures in weld metal (WM) and in HAZ and different levels of strength properties in them. In some HAZ regions of microalloy steel low toughness can be met, with scatter in toughness values.

Many approaches for crack analysis, e. g. EPRI (7), are based on the assumption of material homogeneity. Matching effect must be considered in crack-driving-force (CDF) and residual strength analysis of cracked welded structure for service safety evaluation. The lowest toughness is expected in coarse grains region of HAZ and the crack tip has to be positioned close to fusion line, but when WM is undermatched compared to BM crack tip has to be located in fine-grain region as critical regarding crack resistance.

Positioning of crack tip in the region of lowest toughness is very difficult task and this presents one of important problems in full-scale and model testings for the analysis of results. Crack tip location in specimens can be defined by metallographic analysis for comparison with corresponding location in model or structure.

*University of Skopje, Macedonia
**University of Belgrade, Yugoslavia

TESTING MATERIALS AND SAMPLES

Base material (BM) investigated was high-strength low-alloy (HSLA) steel TStE460, produced by Steelworks Skopje. Chemical composition and tensile properties are given in Table 1.

Table 1. Chemical composition and mechanical properties of TStE460 steel heat

C	Si	Mn	P	S	Cu	Ni	Cr	V	Nb	Al
0.105	0.265	1.63	0.022	0.017	0.22	0.58	0.12	0.105	0.027	0.041
Heat Treatment		Yield strength		Ultimate tensile strength		Elongation				
		R _e , MPa		R _m , MPa		A, %				
Normalization 900°C		445		645		24				
Stress relieving 580°C/ 2 hours		460		625		24.5				

Steel plates 20 mm in thickness were normalized at 900°C after controlled rolling. Testings were performed on models of pressure vessel (1200 mm in diameter, 2600 mm long), on tensile panels of 80x20 mm cross-section and 300 mm referent length and small SEN(B) specimens 20 mm thick. Slight overmatching effect was achieved in submerged-arc-welding (SAW). Chemical composition and mechanical properties of deposited weld metal are given in Table 2.

Table 2 Chemical composition and mechanical properties of SAW deposited TStE460 weld metal

Chemical composition					Yield strength	Ultimate tensile strength	Elongation
C	Ni	Cu	Cr		R _e , MPa	R _m , MPa	A, %
0.1	0.34	0.25	0.11		482	669	18.5

The effect of residual stresses and other influencing factors on the behaviour of pressure vessel containing an axial crack is evaluated through the analysis and tests on samples in as-welded (AW) conditions and after post-welding heat-treatment (PWHT) at 580°C for 2 hours. For comparison, tensile properties of BM after PWHT are presented in Table 1. An artificial crack, 9 mm deep with root radius of 0.1 to 0.15 mm (Fig. 1) had been produced by electrical discharging machine along welded joint, with the intention to position crack tip in HAZ location of similar microstructure in the residual stresses field.

EXPERIMENTAL RESULTSJ integral direct measurement

Approach based on applied crack driving force (CDF), expressed as J_{app} , and material crack resistance, J-R, is used here for residual strength evaluation of cracked pressure vessel. Elastic-

plastic analysis, made by several numerical methods (3,4) is accepted for CDF evaluation of pressure vessels and tensile panels and was verified experimentally through J integral direct measurement on pressure vessel models and tensile panels, as shown in Fig. 2. J integral values for pressure vessels (AW) are higher than for tensile panels TP3 and TP4 (AW), that means for the same J value higher stress is required in tensile panel. Geometrical imperfections are responsible for relative position of J integral dependence for TP3 and TP4 in Fig. 2.

Tensile panels in AW condition start to yield first, TP3 compared to TP1, TP4 compared to TP2, and this is attributed to the contribution of residual stresses. After significant plastification the differences in CDF are reduced. Higher crack resistance of tensile panels TP3 and TP4 can be explained by higher compliance level of pressure vessel PV1. Similar behaviour is observed in elements after PWHT.

The testing of small specimens is much more convenient compared to tensile panels and pressure vessel testing due to its simplicity and cost. The results of small specimens testing are compared to the results of tensile panels and pressure vessel testing for the verification of their applicability in cracked pressure vessel residual strength prediction. Different constraints and compliances due to samples and crack size effects have to be evaluated in addition to the effect of geometrical imperfection. J-R curves and J_{Ic} values are determined according to ASTM E1152 and E813 methods. An average of several test results for specimens with crack tip located in HAZ close to fusion line in region of similar structures amounts $J_{Ic} = 226$ kN/m. Figure 3 presents J resistance curves for three small-size specimens (SS1 and SS2 in PWHT, SS3 in AW condition) compared to J-R curve for TP2 tensile panel in PWHT condition. Similar J-R curve shape for SS2 and SS3 specimens (AW and PWHT) indicates no residual stress effect in both of them. The position of TP2 J-R curve shows that it can be replaced by small specimen J-R curve, but this correspondence must be well proved.

Metallographic investigation

Several samples in AW and PWHT conditions had been grinded, polished and etched (by Nital) for metallographic investigation in order to define exact crack tip location, region of crack growth and corresponding microstructural properties. Crack tip in both investigated samples (PV2 in PWHT, TP3 in AW condition) was found to be in subcritical HAZ (SCHAZ), often referred to as region heated to a temperature below A_{c1} , and some authors define low boundary for SCHAZ as 500-600°C. The crack tip location is visible on the macrograph of PV2 (Fig. 4) and TP3 (Fig. 5) samples, as well as on the micrograph of crack tip region of PV2 sample (Fig. 8). In the figures crack tip is indicated by an arrow. In samples in AW condition similar microstructure is found in this region. It is also visible that crack developed through BM region of SCHAZ, almost parallel to metallographic HAZ boundary up to final fracture, irrespective of sample condition (AW or PWHT).

For the comparison in Fig. 6 and 7 macrographs of PV1 (AW) and TP2 (PWHT) samples are given. One fracture detail is presented in

Fig. 9. The question arose why crack growth path passes through BM region (SCHAZ) and does not touch WM or metallographic HAZ, as it is confirmed in this investigation. In Fig. 10 transition from WM into coarse grained HAZ region is presented with easy to recognize fusion line. In Fig. 11 fine grained HAZ region is shown, and this is in fact SCHAZ and BM boundary in crack growth region (Fig. 9). Clearly visible lamellae, typical for SCHAZ and close BM, are a consequence of high Mn (1.63%) and S (0.017%) contents, producing soft MnS inclusions, elongated in rolling direction. This lamellar structure contributes to base plates anisotropy, followed by microcrack formation (8) and lamellar tearing in plates (Fig. 9). One can conclude that properties of fine grained HAZ region are superior compared to BM, preventing crack development through HAZ.

Microhardness measurement

Microhardness had been measured by Vickers method (2 N loading), in two lines, on distance of 0.5 mm (L1) and 7.5 mm (L1) ahead crack tip on PV2 (PWHT) and TP3 (PWHT) samples. The obtained results are presented in Fig. 12 - 13. Overmatching effect can be recognized: average hardness number in WM area is 230, in BM area 200. The highest values had been discovered in HAZ, in the fusion line vicinity, in coarse grain region. It can be concluded that in both samples (PV2 and TP3) crack tip, being in SCHAZ, is located in high hardness region. The same situation is with all other specimens (PV1, TP1, TP2, TP4). The comparison of differently treated samples (PV2 and TP3) reveals no significant difference in microhardness number, and this was the case with microstructures as well. Accordingly, post-weld heat-treatment (580°C/ 2 hours) does not produce significant differences in hardness and microstructure.

CONCLUSION

The aim of performed investigation was to evaluate the convenience of small-size specimens application for prediction of critical crack driving force and the effect of residual stresses on cracked pressure vessel behaviour. Derived analysis indicates possible application of SEN(B) and TP specimens in residual strength prediction of cracked pressure vessels. Next research could be devoted to the same tests, but with crack tip located in HAZ coarse grained region as critical one in order to compare the results with here presented results. Additional efforts could be directed to specimens with crack transverse to welded joints, with the tip positioned in all critical regions of weldment and base metal.

REFERENCES

- (1) Adžiev, T., Sedmak, S., Petrovski, B., Residual stresses and their effect on J-integral behaviour in full-scale pressure vessel, ICRS-2, Nancy, 1988.
- (2) Adžiev, T., Sedmak, S., Petrovski, B., The effect of residual stresses on residual strength of the welded pressure vessel with an axial notch, in ESIS/EGF Publication 9 "Defect Assessment in Components" - Fundamentals and Applications, Ed. J.G. Blauel, K.H. Schwalbe, Mechanical Engineering Publishers,

- London, 1991, pp.975-985.
- (3) Sedmak, S., Adžiev, T., Crack behaviour in HAZ of small specimens, welded panels and pressure vessels, ICM-6, Kyoto, 1991.
 - (4) Adžiev, T., Sedmak, S., Residual stress effect on crack behaviour in welded panel samples, ICRS-3, Tokushima, 1991.
 - (5) Carlsson, J., Fracture mechanics for cracks in weldments, in "Advances in Fracture Research", pp. 751-762, Pergamon Press, Oxford, 1984.
 - (6) Chao, J. et al, Eng. Fracture Mech., 39, pp. 833-844, 1991.
 - (7) Kumar, V. et al, An engineering approach for elastic-plastic fracture analysis, Electric Power Research Institute (EPRI), 1931, Project 1287-1, Topical Report, 1981.
 - (8) Matrosow, Y.I., Polyakow, i.e., Metallowedenie i termicheskaya obrabotka, 2, 1976, Moscow.

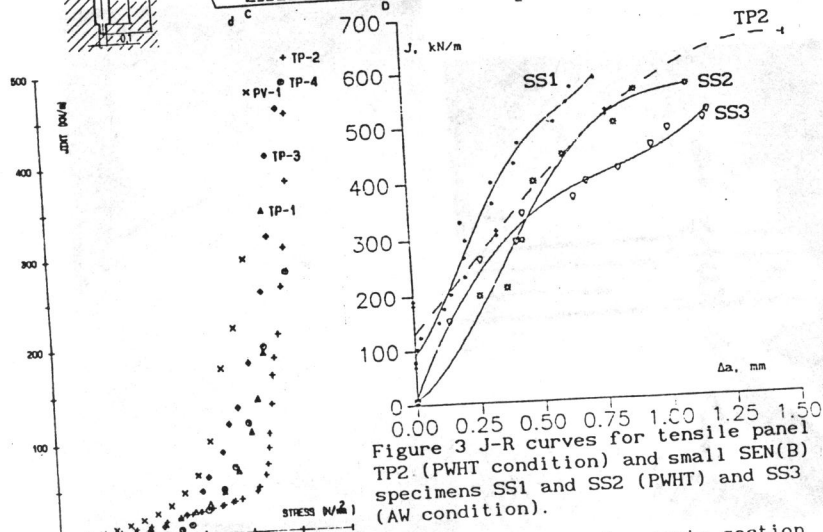
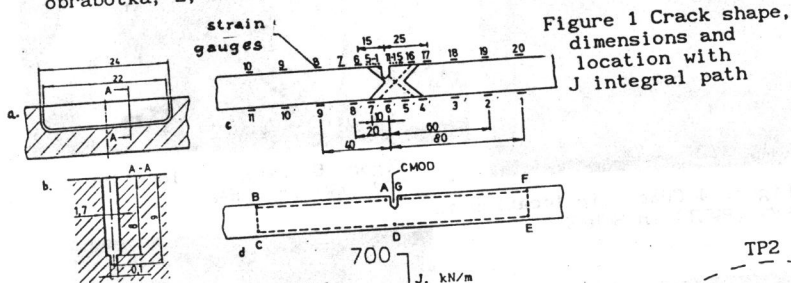


Figure 2 Directly measured J integral vs stress in remote section for pressure vessel PV-1 (AW condition), tensile panels TP1 and TP2 (PWHT condition) and TP3 and TP4 (AW condition).

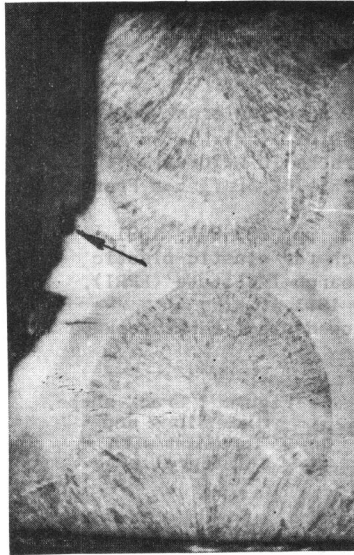


Figure 4 Crack tip location in PV2 (PWHT) in SCHAZ

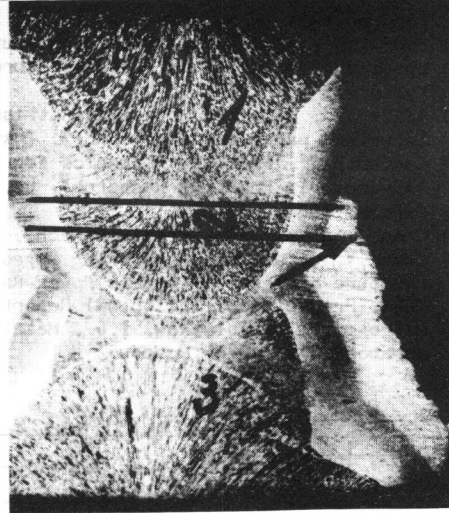


Figure 5 Crack tip location in TP3 (AW) in SCHAZ

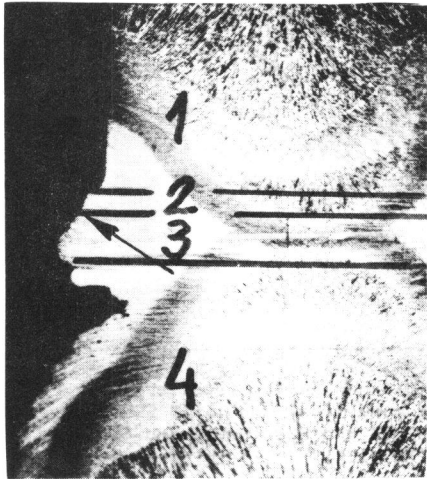


Figure 6 Crack tip location in PV1 (AW)

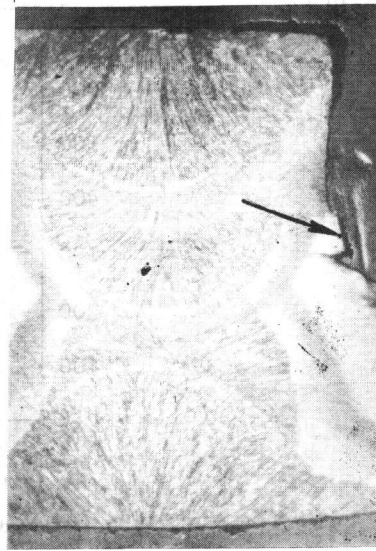


Figure 7 Crack tip location in TP2 (PWHT)

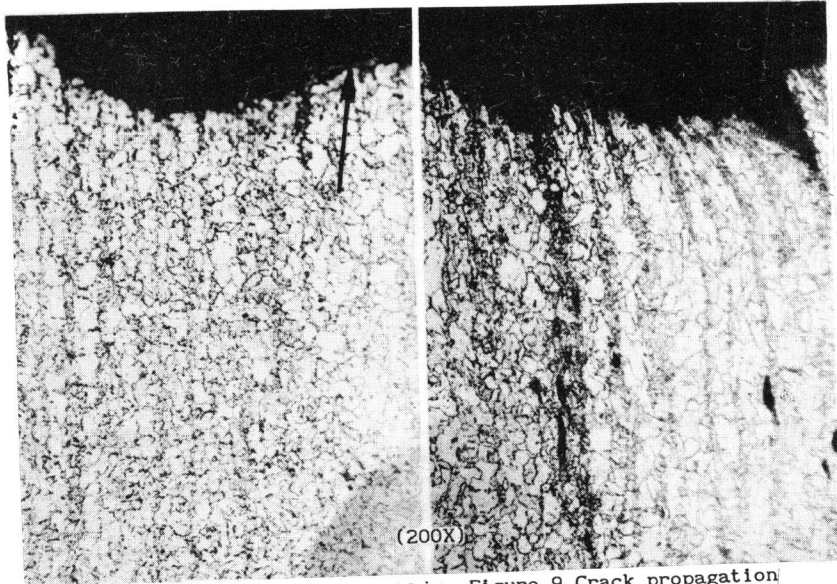


Figure 8 Micrograph of PV2 lamellar structure in crack tip area

Figure 9 Crack propagation through base metal

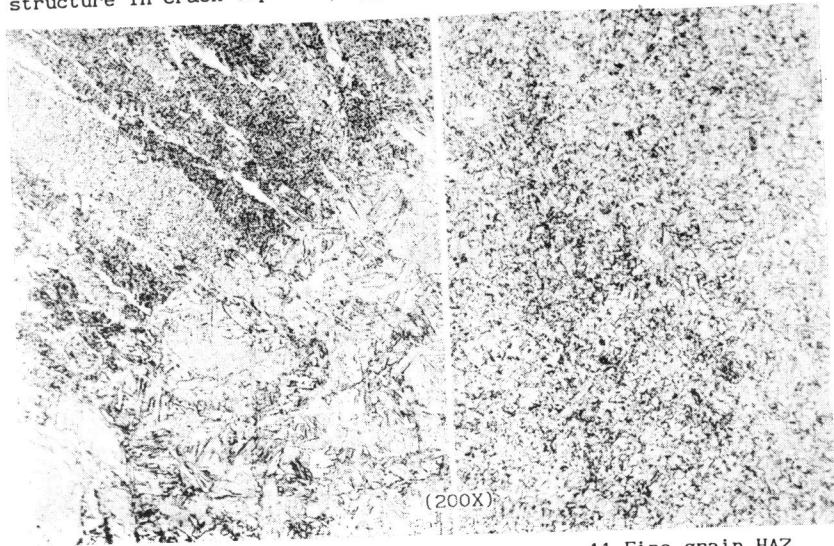


Figure 10 Transition from base metal to coarse grain HAZ region

Figure 11 Fine grain HAZ region

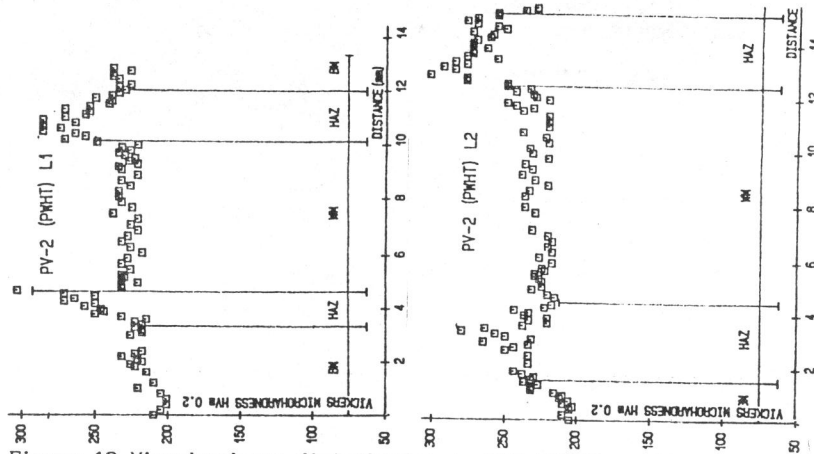


Figure 12 Microhardness distribution in PV2 (PWHT) on line 0.5 mm far from crack tip (L1) and 7.5 mm far (L2)

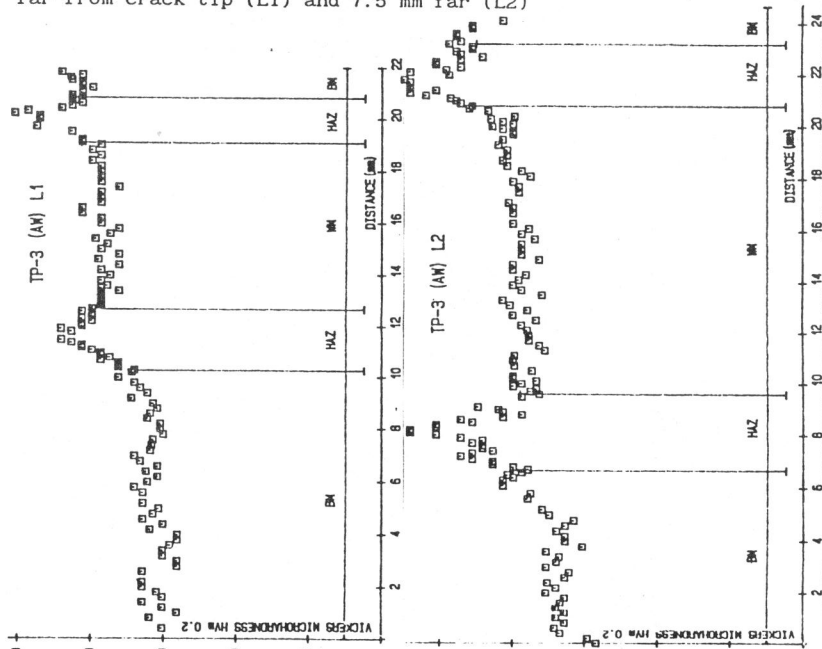


Figure 13 Microhardness distribution in TP3 (AW) on line 0.5 mm far from crack tip (L1) and 7.5 mm far (L2)